PROTEINS: Structure, Function, and Genetics 42:217–229 (2001)

Energy Landscape Theory for Alzheimer's Amyloid β-Peptide Fibril Elongation

Francesca Massi and John E. Straub
Department of Chemistry, Boston University, Boston, Massachusetts

ABSTRACT **Recent experiments on the kinetics of deposition and fibril elongation of the Alzheimer's β-amyloid peptide on preexisting fibrils are analyzed. A mechanism is developed based on the dock-and-lock scheme recently proposed by Maggio and coworkers to organize their experimental observations of the kinetics of deposition of β-peptide on preexisting amyloid fibrils and deposits. Our mechanism includes channels for (1) a one-step prion-like direct deposition on fibrils of activated monomeric peptide in solution, and (2) a two-step deposition of unactivated peptide on fibrils and subsequent reorganization of the peptide–fibril complex. In this way, the mechanism and implied "energy landscape" unify a number of schemes proposed to describe the process of fibril elongation. This β-amyloid landscape mechanism (βALM) is found to be in good agreement with existing experimental data. A number of experimental tests of the mechanism are proposed. The mechanism leads to a clear definition of overall equilibrium or rate constants in terms of the energetics of the elementary underlying processes. Analysis of existing experimental data suggests that fibril elongation occurs through a two-step mechanism of nonspecific peptide absorption and reorganization. The mechanism predicts a turnover in the rate of fibril elongation as a function of temperature and denaturant concentration. Proteins 2001;42:217–229.** © 2000 Wiley-Liss, Inc.

Key words: Alzheimer's disease; Aβ-peptide; fibril; kinetics; reaction rates; denaturant; protein folding

KINETICS OF FIBRILLOGENESIS AND ELONGATION

The crucial role of amyloid peptide deposition as "a necessary but not sufficient factor for the pathogenesis" of Alzheimer's disease has been persuasively argued.[1] Experimental studies of fibril formation and elongation have led to a number of views of amyloidogenesis.[2–4] One view suggests that unstructured monomers in solution cluster and form nuclei.[2] Once the cluster reaches a critical size, the nucleus forms a fibril,[5,6] which then grows to form full-length fibrils by the addition of monomers to the existing fibril ends.[7] In another view, intermediate peptide "protofibrils" are formed[8,9] and associate end-to-end or laterally to form fibrils.[9,10] Subsequently, the amyloid peptide monomer/dimer may add directly to existing protofibrils and fibrils.[11,12] This view may be augmented by the possibility that monomers associate to form micelles and that those micelles may convert to fibril nuclei upon reaching a critical size.[2,5,6]

It has been demonstrated that the process of elongation of existing fibrils through the process of monomer binding to fibril ends can be studied independently of the process of nucleation, micelle conversion, or association of protofibrils[11] (Fig. 1). It is then possible to study the simple, first-order kinetics of fibril elongation[9,12] where

$$\frac{dN_f}{dt} = k_e[m] \tag{1}$$

with N_f the number of peptide monomers in a fibril, k_e is the fibril elongation rate constant, and $[m]$ is the concentration of peptide monomer. By assuming a mechanism of "bimolecular association" of peptide monomer diffusion to the fibril end and activated reorganization of the peptide/fibril, further analysis of the elongation rate constant k_e led to estimates of the separate energy and entropy of activation based on an approximate reaction/diffusion rate constant

$$k_e = D\sigma \exp(-G^\dagger/RT) \tag{2}$$

where σ is the diameter and D is the diffusion coefficient for the peptide monomer.[9,12] The Gibbs free energy of activation can be written in terms of the separate energy, volume, and entropy of activation as

$$G^\dagger = E^\dagger + PV^\dagger - TS^\dagger = H^\dagger - TS^\dagger \tag{3}$$

where the experiments are performed at constant temperature and pressure.

The dimension σ was taken to be on the order of 10 Å, which is roughly the diameter of the monomeric peptide. The diffusion constant for the monomer was taken from experiment to be 1.6×10^{-7} cm^2/s.[12] With a knowledge of k_e and D, experimental analysis assigned a value of $TS^\dagger$ = 16 kcal/mol. When combined with a value of $H^\dagger$ = 23 kcal/mol derived from a van't Hoff analysis, the result is an overall free energy of activation of only $G^\dagger$ = 7 kcal/mol at 300 K. The significant and positive entropy of activation $S^\dagger$ = 0.053 kcal/(mol K) was taken to indicate that the

Grant sponsor: National Science Foundation; Grant sponsor: Center for Computational Science, Boston University.

*Correspondence to: John E. Straub, Department of Chemistry, Boston University, Boston, MA 02215. E-mail: straub@bu.edu

Received 20 July 2000; Accepted 22 September 2000

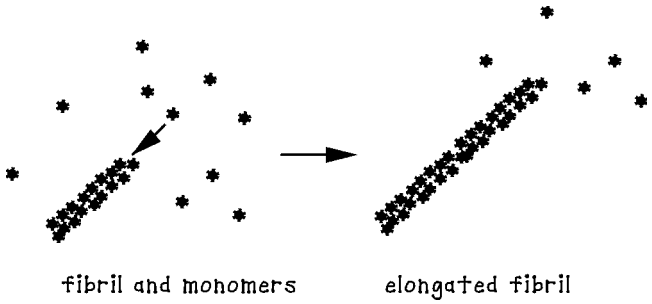

Fig. 1. Kinetics of fibril elongation is first order in the amyloid peptide monomer concentration.

peptide/fibril undergoes an unfolding transition in reaching the transition state from a collapsed, unactivated monomer state.[12]

In demonstrating that fibril elongation occurs by a process of monomer diffusion to the fibril end and subsequent reorganization of the aggregate, these impressive experiments raise questions about the elementary molecular kinetic events of fibril elongation. What is the mechanism of monomer/fibril association? What is the structure of the initial deposit? What is the nature of the reorganization from an initially formed deposit to a well-formed fibril?

A set of key experiments recently performed by Maggio and coworkers[13] partially answer these questions. These investigators explored the kinetics of formation of the "locked" or irreversibly well-formed fibril. A solution of radioactively labeled monomeric peptide in solution was allowed to "dock" onto existing deposits of unlabeled peptide for a loading time τ_L. The deposits were then washed and the off rate for the labeled peptide to leave the deposit was measured. Two well-separated time scales for desorption were observed. The amount of peptide that was found to be "locked" to the deposit such that it would not desorb was found to be a sensitive function of the loading time τ_L. Maggio and colleagues sketched a dock-and-lock scheme in which monomeric peptide diffuses to the fibril end, loads on the deposit, and then undergoes a conformational reorganization to the "locked" state. This scenario is similar to that proposed by Teplow and coworkers.[9,12] However, through their carefully designed experiments, Maggio and coworkers have been able to analyze the kinetics of the association and reorganization steps separately by introducing what they call a "transition state" intermediate of the peptide between the reactant solution state and the irreversibly locked product fibril state. The term "transition state," as used by Maggio and coworkers, refers to a metastable intermediate, rather than the typically unstable activated transition state that appears in the transition state theory of activated processes.

The experimental and interpretive work of these groups has begun to define a reaction mechanism for the process of fibril elongation in terms of elementary molecular processes. In this study, we present a detailed mechanism of fibril elongation that builds on that work. Our kinetic model is used to construct a schematic energy landscape with loosely defined reaction coordinates and transitions states for peptide/fibril association and reorganization. A steady-state kinetic analysis of the proposed mechanism is combined with the experimental data of Maggio and coworkers and is used to assign values to rate constants for the assumed elementary processes of adsorption/desorption and reorganization/deorganization of the amyloid peptide and fibril. A variety of experiments measuring the rate of fibril elongation for mutant and modified forms of the amyloid peptide are interpreted using the proposed energy landscape theory. The result is a kinetic model consistent with existing data that provide a molecular level interpretation of the process of fibril elongation.

ENERGY LANDSCAPE MECHANISM FOR THE KINETICS AND THERMODYNAMICS OF FIBRIL ELONGATION

An important first step in developing a mechanism for fibril elongation is to isolate the reversible and potentially rate limiting steps in the essentially *irreversible* process of fibril elongation. Figure 2 shows a schematic snapshot of the process of fibril elongation including monomeric m peptide in solution, an amorphous deposit of "β" peptide, the reaction interface where the amorphous deposit meets the well-formed fibril, and the β fibril itself. This picture is meant to capture the essence of the dynamics of fibril elongation such as that studied in the experiments of Maggio and coworkers.[13] The dynamics of fibril elongation at lower concentrations is expected to be similar with regard to the reaction interface but may result in less "β" peptide being formed at steady state. At higher concentrations, the loading of layers of "β" peptide is expected to raise the barrier for reorganization of "β" to β peptide at the reaction interface decreasing k_r.

In this simple model, we will assume that the origin of the essentially irreversible formation of fibril is that the peptide adds to existing fibril and then is buried as other peptide is added and the fibril continues to grow. Therefore, while the peptide at the reaction interface shows a reversible reorganization and "deorganization" with rate constants k_r and $k_{d'}$, respectively, once the peptide is buried within the fibril the rate of deorganization $k_{d'}$ is effectively zero. Similarly, in the amorphous deposit the initial adsorption and desorption steps, with associated rate constants k_a and k_d, respectively, are reversible. However, peptide within the β peptide deposit is essentially trapped making k_d effectively zero for those molecules that are not at the interface with the solution. Finally, within the amorphous deposit, "β" peptide that is not at the reaction interface in contact with existing fibril has a rate of reorganization to β peptide k_r that is effectively zero.

The overall picture is one of adsorption/desorption of monomers on the existing deposit and reorganization/deorganization of peptide at the reaction interface. Our proposed mechanism focuses on the dynamics of the association of monomers with the fibril end and the subsequent reorganization step that would be expected to

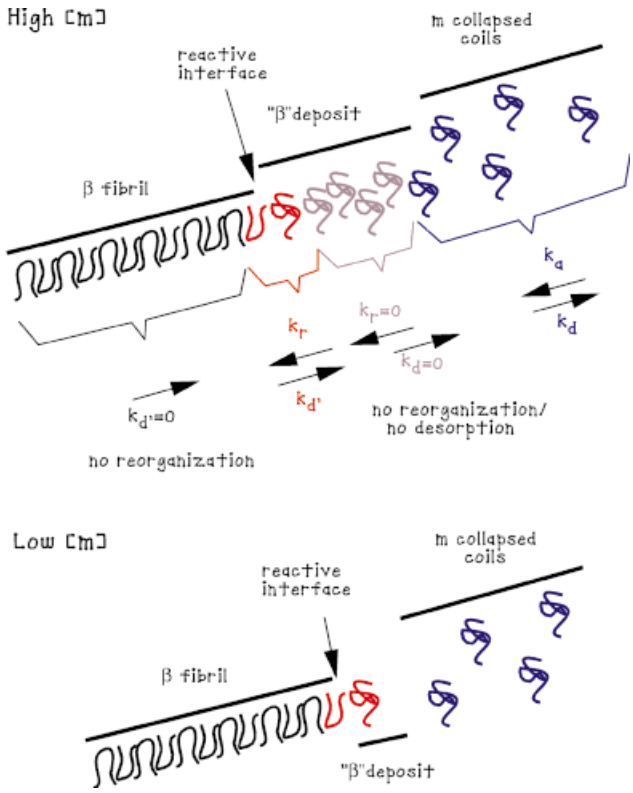

Fig. 2. Schematic "snapshot" of the process of fibril elongation at high and low concentrations of monomeric *m* peptide showing, from right to left, the monomeric peptide in solution; the amorphous deposit of "β" peptide; the reaction interface, where the amorphous deposit meets the well-formed fibril; and the well-formed β fibril itself.

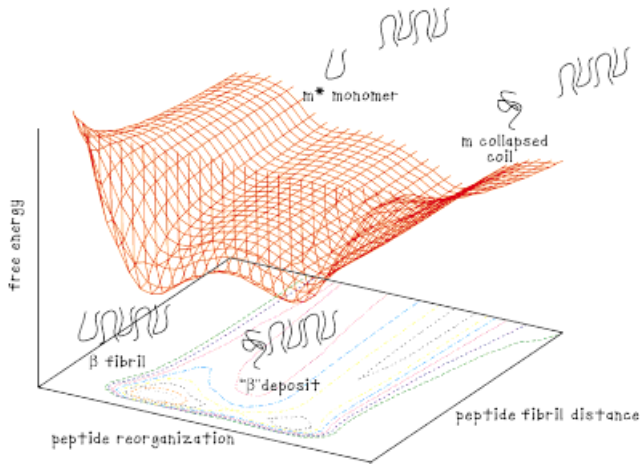

Fig. 3. Schematic energy landscape for amyloid peptide fibril elongation. Depicted on the energy surface are the thermodynamically stable peptide monomer in solution (*m*), the activated monomer in solution (*m**), the amorphous or poorly formed peptide/fibril deposit ("β"), and the well-formed peptide state (β).

represent a steady-state condition at low peptide concentrations.

A simple set of elementary kinetic steps that capture the essential peptide dynamics can be written as follows. The peptide may encounter the fibril end (P) in an unreactive conformation m. In this case, the peptide may deposit itself to the fibril surface to form a poorly annealed extended fibril ("β"). That will occur with a rate k_a for peptide adsorption. Subsequently, the peptide may desorb before the transition from the poorly annealed conformation to the well annealed fibril formation (β) occurs. That will occur with a rate k_d for peptide desorption.

$$m + P \underset{k_d}{\overset{k_a}{\rightleftharpoons}} \text{"β"}$$

After deposition, the peptide, as part of a poorly formed fibril deposit "β," may undergo reorganization and reach the reactive state leading to a secure deposit β before the peptide monomer desorbs. The peptide/fibril reorganization occurs with a rate constant k_r as

$$\text{"β"} \underset{k_{d'}}{\overset{k_r}{\rightleftharpoons}} \beta$$

where $k_{d'}$ is the rate of peptide deorganization. These steps represent a two-step mechanism for fibril formation as deposition of unactivated peptide and subsequent reorganization. A partially structured collapsed coil state encounters the fibril end through diffusion. The peptide deposits itself on the fibril end resulting in a loosely formed deposit. The peptide/fibril deposit then undergoes reorganization to accommodate the peptide in a deposited (product) state. The reorganization step may involve conformational changes in either the peptide or the fibril end, or both. The activation energy for the fibril elongation is associated with peptide/fibril reorganization. Again, at higher concentrations, the loading of layers of "β" peptide is expected to raise the barrier for reorganization of "β" to β peptide, making k_r a decreasing function of time.

It is also possible for the peptide to encounter one of a number of activated transition state conformations m^*

$$m \underset{k_{-1}}{\overset{k_1}{\rightleftharpoons}} m^*$$

If the peptide encounters the precursor fibril end (P) in such a state the deposition is immediately reactive

$$m^* + P \overset{k_a}{\longrightarrow} \beta$$

with a rate constant k_a for peptide adsorption. This is a one-step mechanism of fibril formation as fast deposition of "activated" peptide. A partially structured collapsed coil state of the peptide encounters the fibril end by diffusion. The fibril can be considered frozen, as no fibril end reorganization is required for peptide deposition. The peptide will deposit on the fibril end if, when the peptide encounters the fibril end through diffusion, the peptide is in one of a set of reactive coil conformations. The activation

energy is associated with the peptide monomer reorganization in solution from a set of unreactive configurations to one of a set of transition state configurations.

This model can be interpreted graphically in terms of a dynamics on the amyloid peptide "energy landscape" depicted in Figure 3. The z-axis is a measure of the free energy of the monomer fibril system. The y-axis is a measure of the separation between the peptide monomer and the existing fibril. The x-axis is a coordinate that measures the conformation of the peptide monomer/fibril as it undergoes a transition between the collapsed coil conformation and the β form favored in the fibril. As shown on the landscape, the collapsed coil structure (m) is the predominate thermodynamic form in solution. As the peptide approaches the fibril end along the peptide–fibril separation coordinate it can remain as a collapsed coil and adhere to the fibril end. That structure is the amorphous or poorly formed peptide–fibril deposit ("β"). A slow conformational change of the peptide structure then occurs along the peptide reorganizational coordinate as the peptide reorganizes to the β structure that is energetically favored in the fibril. The well-formed fibril is a thermodynamically stable "global minimum" on the landscape. These steps make up the proposed β-amyloid landscape mechanism (βALM).

Steady-State Rate of Fibril Elongation at Low Peptide Concentrations

Given these two reaction channels, we can examine the overall kinetics. In the general case, the integrated rate laws for the concentration [m], ["β"] and [β] can be determined. Once a steady state of fibril growth is established, the concentration of activated monomer [m*] and poorly annealed monomer added to fibril ["β"] should be constant in time. The result for the steady-state rate of fibril growth is then given by

$$\frac{d[\beta]}{dt} = k_a[P][m]\left(\frac{k_r}{k_r + k_d} + \frac{k_1}{k_{-1} + k_a[P]}\right) - \frac{k_d k_{d'}}{k_r + k_d}[\beta]$$
$$= \zeta_1[m] - \zeta_2[\beta] = -\frac{d[m]}{dt} \quad (4)$$

In the steady-state regime, this model can be solved for the integrated rate of increase of [β] in time as

$$[\beta](t) = [\beta](0)e^{-(\zeta_1+\zeta_2)t} + \frac{\zeta_1}{\zeta_1 + \zeta_2}([m](0) + [\beta](0))[1 - e^{-(\zeta_1+\zeta_2)t}] \quad (5)$$

In the special case in which the initial concentration $[\beta](0) = 0$, $k_{d'}$ is small, making $\zeta_2 \ll \zeta_1$ and $k_1/(k_{-1} + k_a[P])$ is small compared with $k_r/(k_r + k_d)$, we find

$$[\beta](t) = [m](0)\left[1 - \exp\left[-k_a[P]\left(\frac{k_r}{k_r + k_d}\right)t\right]\right] \quad (6)$$

The details of each reaction channel and the conditions under which each channel may predominate are described in the following section. For the purposes of the discussion that follows, we focus on the initial steps in β-fibril elongation and assume that the rate of "deorganization" is small and can be ignored. No such assumption is made in the general form of the βALM mechanism. For each channel, we derive a specific form for the compound elongation rate constant k_e in terms of the elementary rate constants defined by our mechanism.

Fast Equilibrium Formation of Activated m*

Assume that there is a rapid formation of activated monomer in its equilibrium concentration. The rate of deactivation of peptide monomer is assumed to be greater than the rate of adsorption of monomer on precursor fibrils or that $k_{-1} \gg k_a[P]$. In that case the rate law is

$$\frac{d[\beta]}{dt} = k_a[P][m]\left(\frac{k_r}{k_r + k_d} + \frac{k_1}{k_{-1}}\right) \quad (7)$$

Competing pathways for the formation of the well-formed extended fibril β are (1) direct deposition of activated peptide monomer m*, and (2) deposition of unactivated peptide and subsequent reorganization of peptide/fibril. From the definition of the elongation rate constant k_e per deposit or fibril (in units of $\mathrm{L \cdot mol^{-1} \cdot s^{-1}}$) we define

$$\frac{dN_f}{dt} = k_e[m] = \frac{1}{[P]}\frac{d[\beta]}{dt} \quad (8)$$

and find that

$$k_e = k_a\left(\frac{k_r}{k_r + k_d} + \frac{k_1}{k_{-1}}\right) \quad (9)$$

Fast Equilibration with Small $k_1/k_{-1} \ll k_r/k_d$

Assume that there is an equilibrium population of activated peptide monomers (m*) characterized by the equilibrium constant $[m^*]/[m] = k_1/k_{-1}$. The ratio of the reorganization rate constant to the desorption rate constant exceeds the equilibrium constant or $k_r/k_d \gg k_1/k_{-1}$. In such a case, the fibril elongation occurs rapidly as a process of deposition of unactivated peptide and subsequent reorganization depicted in Figure 4. The corresponding rate law is

$$\frac{d[\beta]}{dt} = k_a\frac{k_r}{k_r + k_d}[P][m] \quad (10)$$

The elongation rate constant is given by

$$k_e = k_a\frac{k_r}{k_r + k_d} \quad (11)$$

In the case of $k_d \gg k_r$, the rate is determined by the magnitude of the equilibrium constant for adsorption k_a/k_d and the rate of reorganization of adsorbed peptide. An Arrhenius analysis of the rate of elongation would contain contributions from both the activation energy for peptide/fibril reorganization, as well as the equilibrium free energy of adsorption/desorption

$$G^{\dagger} = G_r^{\dagger} + \Delta G_{\mathrm{eq}}^{a/d} \quad (12)$$

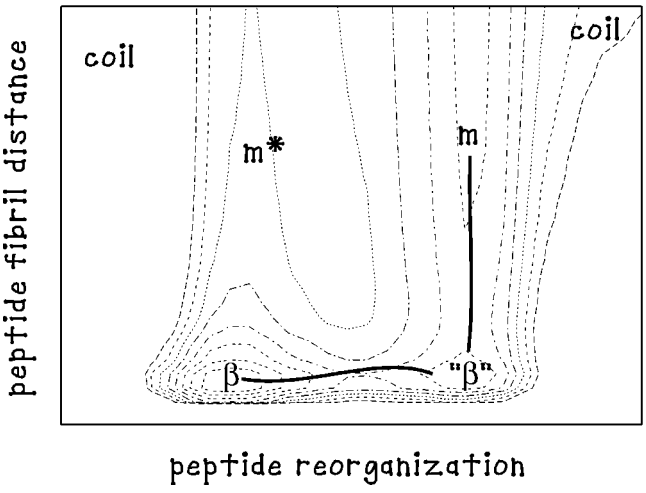

Fig. 4. Schematic energy landscape for amyloid peptide fibril elongation depicting initial adsorption of the peptide in a collapsed coil state, followed by activated reorganization of the peptide/fibril deposit ("β") to access the well-formed peptide state (β).

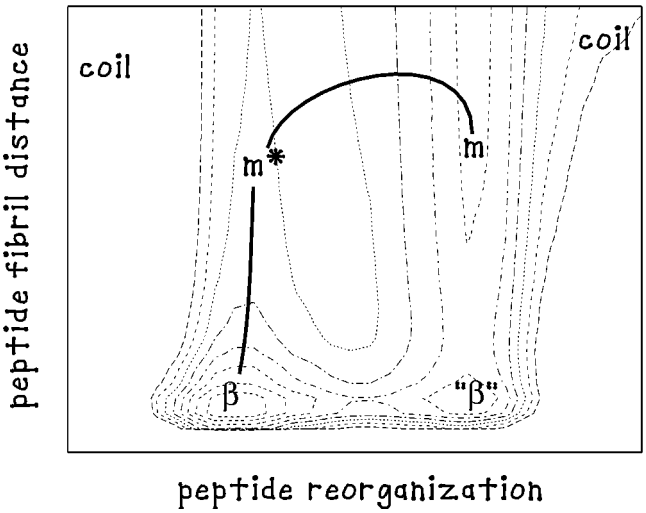

Fig. 5. Schematic energy landscape for amyloid peptide fibril elongation depicting "fast deposition," where the peptide monomer in solution (*m*) accesses a transition state conformation (*m**) that allows for rapid and effectively permanent deposition as well-formed peptide state (β).

In the opposite case of $k_r \gg k_d$, the rate of elongation will reduce to $k_e = k_a$ and the Arrhenius analysis will determine the barrier for the association process $G_a^{\dagger}$.

Fast Equilibrium with Large $k_1/k_{-1} \gg k_r/k_d$

Assume that the ratio of the reorganization rate constant to the desorption rate constant is dwarfed by the equilibrium constant or $k_r/k_d \ll k_1/k_{-1}$. In such a case, the fibril elongation occurs rapidly from the direct deposition of activated peptide as depicted in Figure 5. The corresponding rate law is

$$\frac{d[\beta]}{dt} = k_a \frac{k_1}{k_{-1}}[P][m] \tag{13}$$

The elongation rate constant is

$$k_e = k_a \frac{k_1}{k_{-1}} \tag{14}$$

An Arrhenius analysis of the elongation rate will have a leading contribution from the activation energy for adsorption but will be complicated by contributions from monomer activation equilibrium and peptide reorganization

$$G^{\dagger} = G_a^{\dagger} + \Delta G_{\text{eq}}^{m/m^*} \tag{15}$$

No Significant Formation of Activated *m**

Assume that the activated monomer is rapidly converted to well-formed elongated fibril and

$$\frac{d[\beta]}{dt} = k_a[P][m]\left(\frac{k_r}{k_r + k_d} + \frac{k_1}{k_a[P]}\right) \tag{16}$$

When it is also true that the pathway of direct "nucleation" dominates that of deactivated association and reorganization, which might be the case when the rate of reorganization of adsorbed peptide is slow and $k_1 \gg k_a[P]/(1 + k_d/k_r)$, we find

$$\frac{d[\beta]}{dt} = k_1[m] \tag{17}$$

The rate constant for elongation then becomes

$$k_e = k_1 \frac{1}{[P]} \tag{18}$$

Note that this rate is inversely proportional to the concentration of precursor amyloid deposits [*P*]. When the concentration of precursor deposits is high, an increase in precursor concentration may lead to a slowing of the rate of elongation, as those deposits are competing for scarce monomers.

In this case, the rate is proportional to the rate of activation of the amyloid peptide monomer in solution. In an Arrhenius analysis of the rate constant, the activation energy $G^{\dagger}$ would correspond to the process of conformational reorganization of the solvated peptide. An example would be the opening of the peptide from a tight collapsed coil state.

This simple kinetic scheme serves to demonstrate that the rate constant for fibril elongation may have contributions from a variety of kinetic processes. The take home message is that any Arrhenius analysis must be carefully done to include the contributions from secondary equilibria as well as peptide reorganization on the fibril surface and in solution. Only in the case of direct deposit of activated monomer from solution can we expect to have a "clean" Arrhenius analysis of an activation or equilibrium free energy difference for an isolated elementary process assumed in previous studies.[9,12]

In the next section, we determine the magnitude of the rate constants for peptide reorganization, deorganization and desorption through a fit to experimental data for the rate of peptide deposition measured by Maggio and coworkers.[13]

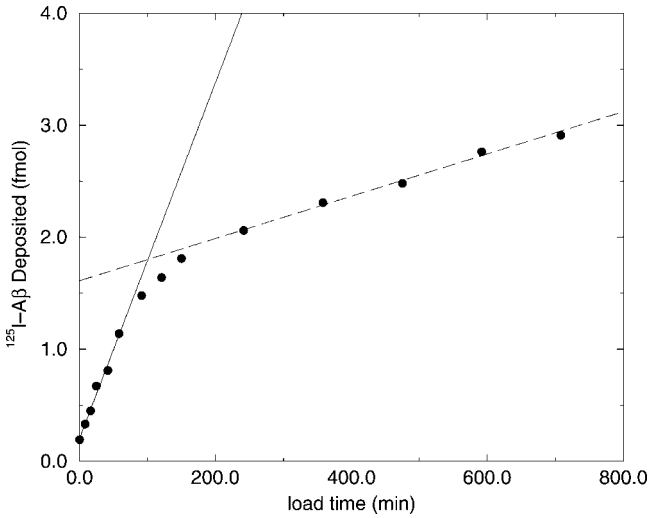

Fig. 6. Absolute quantity of amyloid peptide deposited from solution on synthetic amyloid fibrils is shown as a function of time. The experimental data of Maggio and coworkers[13] is shown with the theoretical fit to the initial rise (with a slope 1.59×10^{-2} fmol/min) and long-time steady-state elongation rate (with a slope 1.89×10^{-3} fmol/min).

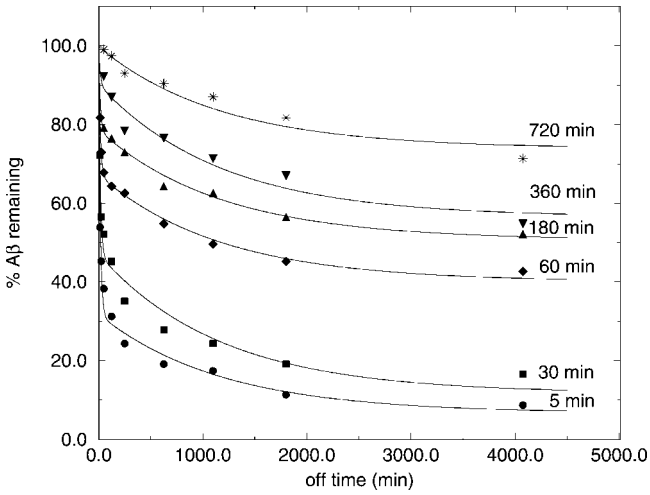

Fig. 7. Fraction of peptide remaining on the deposit as a function of time for a number of values of the loading time τ_L. The experimental data of Maggio and coworkers[13] are shown with the theoretical fit.

ANALYSIS OF EXPERIMENTAL DATA FOR PEPTIDE DEPOSITION AND FIBRIL ELONGATION

Maggio and coworkers,[13] recently carried out a series of experiments that explore the rate of amyloid peptide fibril deposition on existing amyloid deposits. A solution of radioactively labeled amyloid peptide was "loaded" onto existing deposits and allowed to age on the deposit for a loading time τ_L. The deposits were then examined for (1) the quantity of peptide deposited in a given time, and (2) the fraction of peptide that remained on the deposit after the deposit was washed as a function of τ_L. In this section, we use their kinetic data to parameterize the kinetic model proposed above.

Fitting the Rate of Adsorption k_a

In one part of the study of Maggio and coworkers,[13] a fixed concentration of amyloid peptide solution was allowed to interact with preexisting synthetic amyloid fibrils. The amount of peptide deposited as a function of time is presented in Figure 6. The initial rise in the data is assumed to be due to the diffusion limited association of peptide with the existing deposits. Therefore, the slope of the initial rise in the quantity of deposited peptide should be proportional to

$$\text{slope} = k_a[m][P]V \tag{19}$$

where V is the volume of the reaction solution taken to be 1×10^{-4} L (J.E. Maggio, private communication). The fit to the initial rise provides a slope of 0.0159×10^{-15} mol/s. Given that the solution concentration of monomeric peptide was 100 pM = 1×10^{-10} M, we find that $k_a[P]V = 1.59 \times 10^{-7}$ L/s.

Fitting the Rates of Dissociation k_d and "Deorganization" $k_{d'}$

In a second experiment conducted by Maggio and coworkers,[13] the peptide was "loaded" onto a fibril for a time τ_L. The sample was then washed with buffer solution at intervals and the amount of deposited peptide *remaining* was measured as a function of time. This experiment provided "off rates" for the peptide dissociating from the fibril as a function of loading time τ_L. In our mechanism, one expects a fast dissociation of deposited "β" peptide with a rate k_d and a slower dissociation of β peptide that is reorganized with a rate $k_{d'}$. For a sample with a short loading time, the off rate will be dominated by "β" peptide desorbing at a rate k_d. When the loading time is increased, an increasingly large fraction of peptide will have time to reorganize to β. Therefore, an increasingly large fraction of peptide will exhibit an off rate of $k_{d'}$ related to peptide "deorganization." As was done in the experimental study, the data in Figure 7 were fitted to a biexponential of the form

$$\%A\beta \text{ remaining} = A(\tau_L)e^{-k_d t} + B(\tau_L)e^{-k_{d'} t} + C(\tau_L) \tag{20}$$

where $A(\tau_L)$ and $B(\tau_L)$ are the fractions of deposited peptide that correspond to "β" and β, respectively, in our mechanism. The fraction $C(\tau_L)$ is the well-formed β peptide that is "buried" and no longer at the fibril end, where it might deorganize. The fraction $C(\tau_L)$ is effectively irreversibly trapped in the deposit. In this interpretation, the fraction $B(\tau_L)$ is the peptide at the reaction interface. A prediction of our model is that, at steady state, the area of the reaction interface does not depend on time and the fraction of peptide $B(\tau_L)$ should be a constant independent of τ_L. Of course, $A + B + C = 100$. As the reaction interface moves forward, the quantity of peptide at the interface is constant while the peptide in the amorphous

TABLE I. Coefficients A, B, and C[†]

Load time (min)	A	B	C
5	68.2	6.7	25.1
30	53.0	11.7	35.3
60	32.8	40.1	27.1
180	21.4	50.6	27.9
360	9.8	56.5	33.7
720	0.3	73.9	25.8

[†]Fitted values of coefficients A, B, and C as a function of the loading time τ_L.

deposit, initially $A(\tau_L)$, is converted to trapped β peptide, initially $B(\tau_L)$.

In the analysis of their experimental data, Maggio and coworkers identify a "fast" component of peptide that leaves the deposit relatively quickly and a "slow" component of peptide that leaves the deposit slowly or not at all. The "fast" component is essentially the loosely held "β" peptide of the amorphous deposit with an initial fraction $A(\tau_L)$. However, no distinction was made regarding the peptide at the reaction interface and the peptide trapped in the deposit that we assign to initial fractions $B(\tau_L)$ and $C(\tau_L)$, respectively. Both fractions were said to constitute the "slow" component. Our analysis makes it clear that the fraction $B(\tau_L)$ of peptide at the reaction interface is independent of the loading time and the conversion of "fast" to "slow" components is a conversion of $A(\tau_L)$ to $C(\tau_L)$ that occurs as the reaction interface moves outward in the process of fibril elongation.

We find that a best fit is obtained with $k_d = 6.7 \times 10^{-2}$ min^{-1} and $k_{d'} = 8.5 \times 10^{-4}$ min^{-1} and the coefficients showing in Table I.

These values of the rates for dissociation and deorganization can be compared with the time constants for the biexponential fits of Maggio and coworkers, using a functional form $Y = [A \exp(-k_1 t) + (1 - A)\exp(-k_2 t) + C]/(1 + C)$ and values of $t_{1/2} = \ln(2)/k_1 = 10.4 \pm 2.1$ min or $k_1 = 6.6 \times 10^{-2}$ min^{-1} and "the half time for the second (slower) dissociation process was at least 100-fold longer".[13]

Fitting the Rate of Reorganization k_r

The reorganization of the deposited peptide is the rate-limiting step in the conversion of the "β" to β peptide form. Figure 8 shows the relative fractions of deposited peptide as a function of the loading time τ_L. We expect that the rate of interconversion of the fraction $A(\tau_L)$ to $C(\tau_L)$ of "β" to β will vary as the sum of the rate of reorganization and deorganization $k_r + k_{d'}$.

In the experiment, what is measured is the reorganization of the newly deposited peptide. Peptide that was part of the deposit before the loading began is not labeled and not counted in the statistics. The first step is to populate the fibril with labeled peptide. Once a site is covered with labeled peptide, there is a chance that the amorphously deposited peptide "β" will convert to the well-formed β. That occurs with a probability

$$\text{Probability of reorganization} = e^{-(k_r + k_{d'})\tau_L} \qquad (21)$$

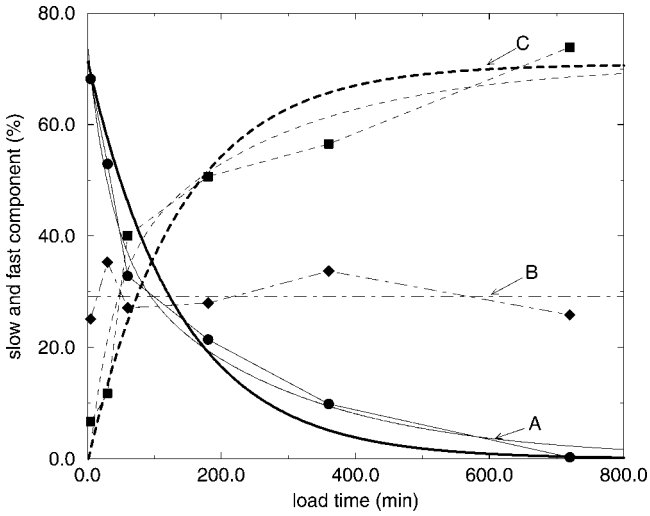

Fig. 8. Relative fractions of the A (amorphous deposit), B (reaction interface), and C (buried fibril) components in the experiments of Maggio and coworkers[13] load time τ_L. The experimental data[13] are shown with the theoretical single exponential (dark curves) and double exponential (light curves) fits to our model.

We expect that $k_r \gg k_{d'}$ so that the observed rate of propagation of the reaction interface can be taken to be the rate of reorganization k_r. This allows us to fit the fraction of β (fast) and "β" (slow) peptide, using the approximation

$$A(\tau_L) = A(0)e^{-k_r \tau_L} \qquad (22)$$

and

$$C(\tau_L) = C(0)[1 - e^{-k_r \tau_L}] \qquad (23)$$

These general fitting functions provide us with an estimate of the rate of reorganization as well as an estimate of the diffusional association rate. The fit based on the value $k_r = 7.3 \times 10^{-3}$ min^{-1} is shown in Figure 8.

While the single exponential fit captures the essential features of the loading time dependence of the relative fractions of deposited peptide, a more accurate fit can be obtained using a biexponential or stretched exponential time-dependent model. For example, using a biexponential time dependence, the relative fractions of A, B, and C peptide are fitted to $A(\tau_L) = 35.7 \exp(-2.9 \times 10^{-2}$ min^{-1} $\tau_L) + 39.1 \exp(-3.9 \times 10^{-3}$ min^{-1} $\tau_L)$, $B(\tau_L) = 29.2$ and $C(\tau_L) = 100 - A(\tau_L) - B(\tau_L)$) also shown in Figure 8. The stretched exponential fit of the form $A(\tau_L) = 82.0 \exp(-0.068$ min^{-1} $\tau_L^{\gamma})$, where $\gamma = 0.59$ is similar in appearance. The goodness of the biexponential or the stretched exponential fits to $A(\tau_L)$ may be taken to indicate the presence of a distribution of barriers for the conversion of "β" to β-peptide.

Using the fits to the relative fractions of peptides we can compute the absolute quantities of peptide in the "β" phase within the deposit (A), the "β" phase at the reaction interface (B), and the β phase of the well-formed fibril away from the interface (C). The results are shown in Figure 9. Initially, there is an increase in the concentration of peptide in the amorphous deposit and at the

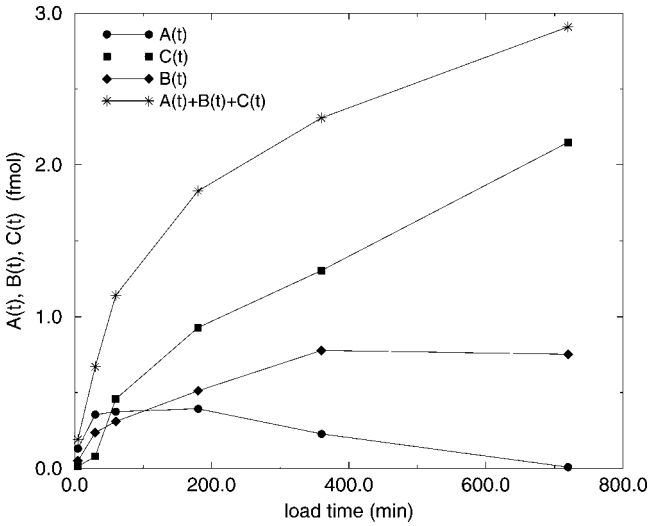

Fig. 9. Absolute quantities of the *A* (amorphous deposit), *B* (reaction interface), and *C* (buried fibril) peptide components derived from our model applied to the experimental data of Maggio and coworkers.[13]

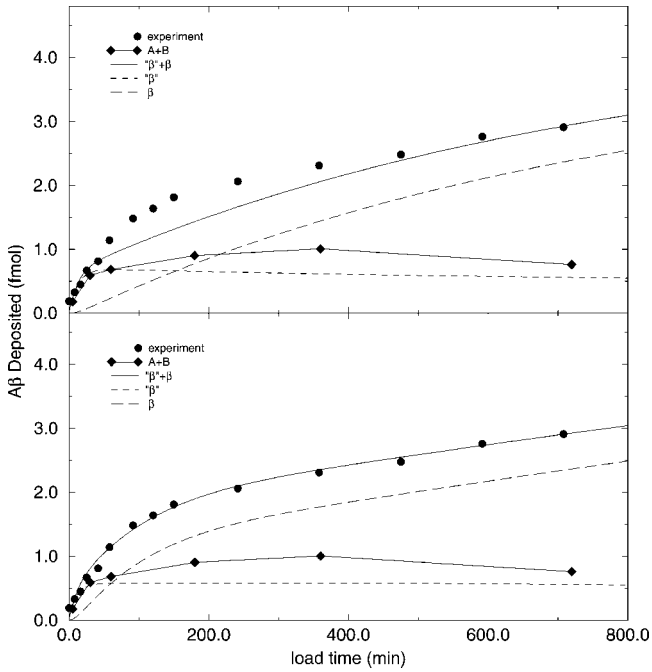

Fig. 10. Absolute quantities of the "β" (amorphous deposit and reaction interface), and β (buried fibril) peptide components derived from the βALM kinetics are shown with the experimental data of Maggio and coworkers.[13] Top, results for a time-independent $k_r = 0.0073\ \text{min}^{-1}$. Bottom, results using a time-dependent $k_r(t) = (0.0185\ \exp(-k_a[P]t) + 0.0069)\ \text{min}^{-1}$, where $k_a[P] = 0.00556\ \text{min}^{-1}$.

reaction interface. The rate of increase is determined by the rate of peptide diffusion to the fibril ends. Subsequently, there is an increase in the quantity of peptide in the fibril—the "irreversibly" formed fibril. The rate of increase is determined by the rate of peptide reorganization at the reaction interface. The sum total of the three components is the total quantity of peptide added to the fibril as a function of time (Fig. 6).

Another test of this mechanism is to predict the rate of increase of β-fibril shown in Figure 6 by directly solving the differential rate laws of the β-amyloid landscape mechanism proposed here for $\beta(t)$. The results based on the rate constants k_aP, k_d, $k_{d'}$ and time-independent $k_r = 0.0073\ \text{min}^{-1}$ are shown in the upper panel of Figure 10. Overall, the general features of the increase in deposited peptide are captured by the proposed β-amyloid landscape mechanism (βALM). While the values of the elementary rate constants should be somewhat independent of the concentration of monomeric peptide in solution, the kinetics of peptide deposition is more complex at high peptide concentrations (Fig. 2). At higher concentrations, it is expected that the rate of reorganization of deposited peptide will depend on the surrounding deposit with the rate of reorganization decreasing as the steady-state thickness of the deposit is increased. In the lower panel of Figure 10, the kinetics resulting from the use of a time dependent $k_r(t) = [0.0185\ \exp(-k_a[P]t) + 0.0069]\ \text{min}^{-1}$ where $k_a[P] = 0.00556\ \text{min}^{-1}$ is shown. Note that for the rate of decrease in the rate we have used the rate of peptide association from solution. The fit is in excellent agreement with the experimentally measured rate of increase in the deposited peptide.[13]

In the next section, we suggest forms for the absolute rate constants for bimolecular reaction/diffusion and unimolecular conformational reorganization that appear in the elementary steps of the energy landscape mechanism.

ABSOLUTE REACTION RATE CONSTANTS FOR REACTION/DIFFUSION AND UNIMOLECULAR CONFORMATIONAL TRANSITION

The rate constants that appear in the proposed two channel mechanism can be modeled as a "bimolecular" reaction/diffusion of peptide and deposit and "unimolecular" reorganization of the peptide and peptide/deposit. Specific forms of the elementary rate constants are developed in this discussion.

Peptide Reaction/Diffusion in Deposition from Solution

The Smoluchowski rate theory provides an estimate of the equilibrium flux for the formation of contact between two species P and m of radii σ_P and σ_m diffusing in solution with a relative diffusion coefficient $D = D_P + D_m$. The rate constant for association is simply

$$k_a^D = 4\pi D\sigma\alpha \tag{24}$$

where $\sigma = \sigma_P + \sigma_m$ is the contact radius. These features are summarized in Figure 11. The parameter α is a measure of the probability that on contact the peptide deposits on the fibril. It has been shown that the monomer of the amyloid peptide congener in aqueous solution has a large hydrophobic surface area A_H.[16,17] If we take the peptide to have a total surface area $4\pi\sigma_m^2$, we expect that the probability that on approach the peptide will be

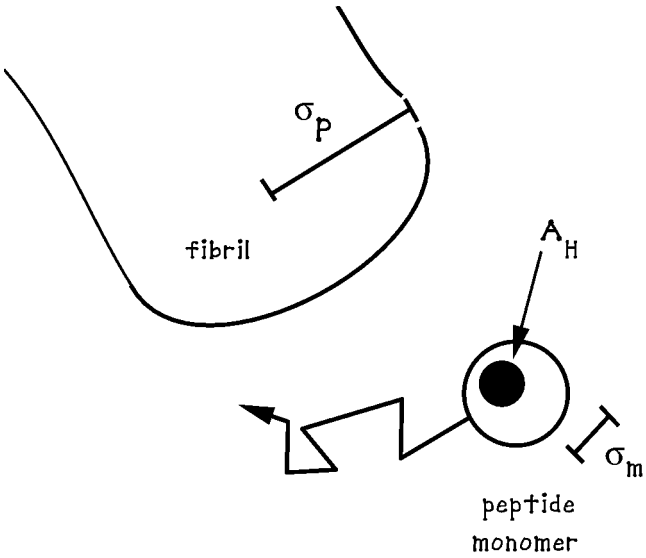

Fig. 11. Schematic of the diffusive encounter of a peptide monomer and an amyloid fibril indicating the exposed hydrophobic surface area A_H.

reactive and deposit on the amyloid fibril will be proportional to

$$\alpha = \frac{A_H}{4\pi\sigma_m^2} \tag{25}$$

In many cases, the formation of a contact is not enough for a reaction to occur. It is also necessary to have the species in contact overcome an activation energy barrier to form product. If the activation barrier is $G_a^\dagger$ the Debye–Smouchowski rate constant for reaction is simply the rate of forming a contact times the probability of the reactant being activated at the time the contact is formed or

$$k_a^{DS} = 4\pi D\sigma\alpha \exp(-G_a^\dagger/RT) \tag{26}$$

We expect that the attractive energy that encourages the peptide to bind to the fibril will also be proportional to the exposed hydrophobic surface area A_H as

$$\Delta G^{a/d} = \epsilon A_H \tag{27}$$

where ϵ is on the order of hundredths of RT per Å^2 of exposed hydrophobic surface area. To a first approximation, this energy scale determines the equilibrium constant for the adsorption/desorption equilibrium.

From a fit to the data of Figure 6, we find that $k_a[m][P] = 0.0159$ fmole/min $= 2.6 \times 10^{-19}$ mol/s, where the concentration of monomeric peptide is $[m] = 1 \times 10^{-10}$ M. Therefore, for a volume of 1×10^{-4} L of solution we find $k_a[P] = 2.6 \times 10^{-5}$ s^{-1}. The estimated number of fibril ends is $[P] = 1 \times 10^{-9}$ mol/1×10^{-4} $L = 1 \times 10^{-5}$ M.[15] However, in experiments of Maggio and coworkers one expects that many of the fibril ends will be covered or relatively inaccessible. Therefore, the number of readily accessible fibril ends is expected to be something less than 1 nmole.

We can make a quick estimate of the number of fibril ends readily accessible to the diffusing monomers. Suppose that the association process has a rate constant is $k_a = 4\pi D\sigma\alpha \exp(-G_a^\dagger/RT)$. The exposed hydrophobic patch has been estimated to be on the order of 600–1000 Å^2 for the peptide of total solvent exposed surface area of roughly 3600 Å^2.[15] That leads to a value of $\alpha = 0.2$. Using a value of $D = 1.4 \times 10^{-6}$ cm^2/s,[15] a reaction diameter of $\sigma = (\sigma_P + \sigma_m) = 2 \times 10^{-7}$ cm leads to an estimate of $k_a[P] = 4.2 \times 10^8 \exp(-G_a^\dagger/RT)$ L/(mol s) $[P]$. Our estimate, then, is that

$$\exp(-G_a^\dagger/RT)[P] = 7.2 \times 10^{-9} \tag{28}$$

"Unimolecular" Peptide and Peptide/Fibril Conformational Transitions

The "reaction coordinate" for the reorganization of peptide/fibril may be defined in terms of the peptide reorganization alone, fibril reorganization alone, or a combination of peptide/fibril reorganization. The standard theory for describing such an event is the transition state theory.[17–19] The transition state theory estimate of the rate constant can be written

$$k_{TST} = \nu \exp(-G_r^\dagger/RT) \tag{29}$$

where the free energy of activation $G_r^\dagger$ determines the statistical probability of accessing the transition state conformation, and the prefactor is a measure of the equilibrium flux of activated reactants across the transition state.

Transition state theory assumes that every reactant that accesses the transition state will necessarily react and form product. It may be that the system dynamics will cause the activated reactant to undergo (1) inertial oscillation back to reactant or (2) collisions that return the activated state to a reactant state. In either case, the actual rate constant will be $k = \kappa k_{TST}$ where $0 \le \kappa \le 1$ is the transmission coefficient, which accounts for those dynamic recrossings. Dynamic recrossings only serve to lower the reaction rate making the *TST* rate constant an upper bound to the true reaction rate constant (see below).

A van't Hoff analysis of the individual steps of association and reorganization is necessary to determine the contributions of activation enthalpy and entropy to the peptide/fibril conformational transition. In our proposed mechanism, the overall rate constant for fibril elongation is a composite of the elementary rate constants for peptide/fibril association and reorganization. A van't Hoff analysis of the temperature dependence of the overall rate constant will not, in general, provide the activation enthalpy for the elementary molecular processes alone. However, a van't Hoff analysis of the individual steps observed in the experiments of Maggio and coworkers[13] will make such an assignment possible.

COMPARISON WITH EXPERIMENT: EFFECT OF MUTATION AND CROSSLINKING ON FIBRIL ELONGATION

The proposed energy landscape model of fibrillogenesis can be used to organize a variety of experimental observa-

tions of the rate of elongation and growth of amyloid fibrils for a variety of modified forms of the amyloid β peptide and a congener. In this discussion we focus on experiments on the Aβ(1–40) peptide and a truncated congener Aβ(10–35)—NH_2, which has been shown to be a good model of the full Aβ peptide in plaque competence and deposition assays.[16,21]

Wild-Type Congener Aβ(10–35)—NH_2

The WT peptide congener has been shown to exist in a loosely formed collapsed coil state in aqueous solution.[21,22] The structure of the collapsed coil is characterized by a central hydrophobic cluster in the LVFFA (17–21) region. There is also a dominant turn in the VGSN (24–27) region, which is observed in both the aqueous solution structure[15] and the TFE–water solution structure,[22] also studied in dimethylsulfoxide (DMSO), which shows two short α-helical regions. Analysis of the exposed hydrophobic surface area of the collapsed coil structure[14] shows that the peptide presents a large fraction of hydrophobic surface.

In the model above, the large hydrophobic surface increases the value of the equilibrium constant k_a/k_d for the adsorption/desorption of the peptide monomer on the amyloid deposit. The collapsed coil structure is also expected to be a low-lying intermediate with a reduced free energy barrier to adsorption relative to the unstructured coil state (Fig. 3).

Wild-Type *A*β(1–42) and *A*β(1–40) Peptides

It has been shown that the *A*β(1–40) peptide deposits more slowly than the *A*β(1–42) peptide. This points to the importance of the C-terminus in affecting the formation of seeds by the amyloid peptide.[23] The rate of deposition of the peptide is approximately a factor of two larger in the case of the *A*β(1–42) relative to the *A*β(1–40).

In the energy landscape mechanism, it is unclear whether the change in the C-terminus affects the rate of association k_a through a change in the solution structure of the peptide or a change in the rate of reorganization k_r of the deposited peptide, or both.

Wild-Type D- and L-Aβ(1–40) Peptides

Studies of the D- and L-stereoisomers of the *A*β peptide have shown stereospecificity in the fibril elongation process.[26] It was shown that L-*A*β(1–40) peptide deposited on L-*A*β(1–40) peptide templates with a first-order kinetic dependence on the concentration of peptide monomer in solution. It was also shown that D-*A*β(1–40) peptide would deposit onto the D-*A*β(1–40) peptide template according to a rate that was first order in the peptide concentration. However, no fibril elongation of L-*A*β(1–40) peptide on D-*A*β(1–40) peptide template, or D-*A*β(1–40) peptide on L-*A*β(1–40) peptide template, was observed. These experiments demonstrate that the elongation process is similar in both peptide enantiomers, as long as the depositing peptide and the existing template are of similar chirality. When the chiralities differ, the deposition does not occur.

In the energy landscape theory proposed here, we expect that the association process and k_a would be largely unaffected by the change in chirality of the peptide. This would be true if we assumed that the solution conformation of the peptide enantiomers were similar in size and exposure of hydrophobic surface. However, the reorganization process could be quite different if the chirality of the depositing peptide and existing template differed. In that case, the conformations required to make a well-formed deposit may not be accessible to the peptide rendering k_r effectively equal to zero.

Less Restrained Dutch Mutant *A*β(10–35)—NH_2—E22Q

Experimental analysis of the Dutch mutant of the WT amyloid peptide has shown the mutant to be significantly more active than the WT peptide with a twofold increase in the rate of fibril elongation and deposition competence.[13] Experimentally determined H_α chemical shifts in the WT and Dutch mutant indicate that the structures of the monomeric peptides in solution are similar.[13] The increased deposition rate observed for the Dutch mutant has been explained in terms of a more disordered solution state relative to the WT peptide.[13] The looser structure is believed to lower the entropic barrier for "opening" of the peptide, which is necessary in the reorganization process.

In the energy landscape mechanism proposed in this discussion, we would expect to see in the E22Q mutant an enhanced value of k_a as a result of the replacement of the charged glutamate residue with a polar glutamate residue lowering the desolvation barrier in adsorption. The greater flexibility in the peptide may also lead to a reduced barrier to reorganization and a larger k_r, producing a greater rate of fibril elongation.

More Restrained Cyclic Crosslinked *A*β(10–35)—NH_2-CycloH14K–E22 Peptide

Experimentally measured H_α chemical shifts in the cyclic peptide indicate that the structure of the monomeric peptide is similar to the structure of the WT peptide.[36] Nevertheless, the cyclic mutant peptide is found to be inactive in deposition. This has been interpreted as a demonstration that the peptide must be allowed to access an "open" or extended conformation in order to add to a well-formed amyloid deposit.

In the mechanism described above, we would expect that if the exposed hydrophobic surface area is similar in the cyclic peptide and the WT peptide, the cyclic peptide would adsorb on the fibril. However, the peptide would be unable to reorganize to access conformations consistent with a well-formed amyloid deposit. Therefore, we might expect the value of k_a to be similar for the WT and cyclic peptides while the values of k_r and k_1 would be essentially zero for the cyclic peptide. The cyclic peptide would be capable of adsorption on the existing amyloid deposit but would be easily washed off of the deposit as the peptide/fibril would not be able to reorganize to a conformation consistent with the well-formed β fibril.

Disrupted Central Hydrophobic Cluster of $A\beta(10–35)$-NH_2-F19T

NMR structural analysis of the F19T mutant of the amyloid peptide congener in aqueous solution indicates that there is a serious disruption of peptide structure in the central hydrophobic cluster (CHC) region of the mutant peptide. This disruption of the CHC is correlated with a diminished ability of the peptide to add to well-formed amyloid deposits.

In both the F19T mutant and the E22Q Dutch mutant the amyloid peptide monomer in solution is found to be less constrained in the coil state. However, in the case of the E22Q Dutch mutant and the WT peptide, the structure of the CHC is preserved.

In the mechanism proposed here, we would find that in the F19T mutant the ability of the peptide to adsorb would be significantly diminished due to a reduced hydrophobic surface area A_H and adsorption rate constant k_a.

DEPENDENCE OF THE ELONGATION RATE CONSTANT K_E ON DENATURANT CONCENTRATION, TEMPERATURE, AND SOLVENT VISCOSITY

The proposed mechanism makes predictions of a specific temperature dependence in the rate of fibril elongation.

Turnover in Rate of Fibril Elongation With Increasing Denaturant Concentration

Experiments[25,26] have shown that the addition of denaturant can increase the rate of protein folding by reducing the time spent in misfolded intermediate states. The addition of denaturant is expected to impact two elementary steps in the energy landscape mechanism. The denaturant will favor a less structured collapsed coil state.[27,28] This may decrease the diffusion constant for the peptide monomer. It is also expected that the less structured peptide will be able to reorganize more readily lowering the barrier to reorganization and increasing the rate constant for reorganization. If that is the dominant effect, the rate of reorganization and the addition of denaturant should increase the rate of fibril elongation.

At high enough concentrations of denaturant the structure of the collapsed coil state will be severely destabilized and the monomers will be predominantly unstructured coil states. This should lead to a decrease in the diffusion constant for the peptide monomer and a decrease in the rate of adsorption.[15]

Overall, we expect that as the concentration of denaturant is increased there will be a "turnover" in the rate of elongation k_e. This effect is shown schematically in Figure 12.

In earlier experiments of Maggio and coworkers[29] preliminary evidence for such a turnover was reported in the rate of amyloid peptide deposition as a function of urea denaturant concentration.

Turnover in Rate of Fibril Elongation With Increasing Temperature

At lower temperatures, experiments have found the collapsed coil states to be stable relative to largely random coil states.[20] In the 5–35°C range, we expect that a temperature increase will increase the rates of association and reorganization due to an increase in the probability of being found in an activated state in the reaction/diffusion or reorganization process. Increasing temperature should also "loosen" the collapsed coil state and, at lower temperatures, increase k_e.

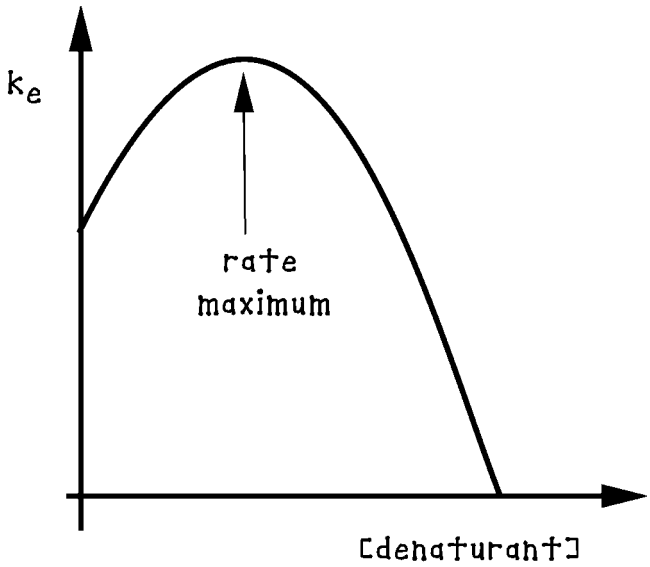

Fig. 12. At low denaturant concentrations, the elongation rate increases due to a lowering of the activation energy for conformational transitions in the collapsed and adsorbed peptide. At high concentrations of denaturant, the elongation rate decreases due to a destabilization of the collapsed coil states and a decrease in peptide adsorption to amyloid deposits. At intermediate concentrations, there is a turnover and maximum in the elongation rate constant k_e.

At higher temperatures the collapsed coil state will become destabilized relative to the random coil states. This will eventually deteriorate the ability of the peptide to associate with the amyloid deposit (an effect similar to that induced by high concentration of denaturant). The result should be a decrease in the rate of association and lead to an overall decrease in k_e with increasing temperature.

Overall, with increasing temperature we expect to see an initial increase in the rate of amyloid deposition and fibril elongation followed by a "turnover" and decrease at high temperatures.

Rate of Fibril Elongation Decreases With Increasing Solvent Viscosity

For the energy landscape mechanism proposed, the rate constants for reaction/diffusion and reorganization can be parameterized through experiment and simulation to account for the various elementary reaction processes described in the two channel mechanism for amyloid fibril elongation. The rate constant k_a is expected to be a strong function of the solvent viscosity. An increase in solvent viscosity η will decrease the diffusion constant $D = RT/\gamma$ through an increase in the friction $\gamma = 6\pi\eta r_H$, where the peptide hydrodynamic radius is r_H. The rate of peptide

reorganization is expected to be a comparatively weak function of the solvent viscosity. Therefore, we expect the elongation rate k_e to be a monotonically decreasing function of the solvent viscosity.

DISCUSSION OF PROTEIN FOLDING AND MISFOLDING AND THE RELATION TO *A*B PEPTIDE DEPOSITION

One view of amyloid peptide fibril elongation suggests that the solution phase of the amyloid peptide monomer is largely unstructured and samples a large number of disordered coil states on the time scale of fibril elongation. Fibril elongation follows a mechanism of peptide adsorption and subsequent peptide/fibril reorganization. Another view suggests that the conformation of the peptide monomer in solution is a crucial determinant of the rate of fibril elongation. The latter view has led to suggestions that theories of protein folding may elucidate aspects of the mechanism for fibril elongation.[14,30]

What can be learned from the analysis of amyloid peptide fibrillization as a protein folding problem? Modern theories of protein folding have been successful in organizing a significant volume of experimental data for folding stability analysis and kinetics. In the best case, they have not only provided a means of "organizing one's thinking" about the problem, but a framework for predicting unobserved behavior and suggesting novel experiments as well.[28,31–35] An obvious and suggestive isomorphism exists between the processes of protein folding and amyloid fibril elongation.

The kinetic process by which the protein arrives at the native state may follow one of two mechanisms. Both mechanisms follow a three-stage pathway of (1) collapse from a largely unstructured coil state to a compact state, (2) search through a set of compact states for a transition state, and (3) folding to the native state. The process is depicted for the case of the amyloid peptide in Figure 3, where it is imagined that the compact state is represented by a collapsed coil state and the "native" state of the protein corresponds to the peptide in a well formed amyloid deposit.

In the kinetic partitioning mechanism (KPM) of protein folding[33] proposed by Thirumalai and coworkers,[31] it is assumed that a certain fraction of proteins follows a fast folding process through a nucleation-collapse mechanism, while the remaining fraction folds to a non-native compact intermediate or misfolded state and subsequently overcomes an energetic barrier to "reopen" and fold to the native state. The energy landscape mechanism for amyloid peptide deposit proposed can be considered isomorphic with this KPM.

"Fast Folding" and "Fast Deposition"

In the kinetic nucleation–collapse process, the protein searches for a set of critical contacts and, upon forming that critical "nucleus," folds rapidly to the native state. In the kinetics of amyloid peptide deposition, it has been proposed that an activated or "transition state" conformation of the *A*β peptide monomer can be found that is rapidly and well deposited on an existing fibril. That process of "fast deposition" corresponds to the direct nucleation mechanism by which a protein may access its native state.

Misfolded Intermediates and Poorly Formed Amyloid Deposits

A fraction of proteins do not follow an efficient nucleation-collapse mechanism but instead initially misfold into a low energy but non-native compact state. These proteins undergo an activated transition to escape the misfolded state and refold to the native conformation. In the energy landscape mechanism for fibril elongation proposed, the process of deposition of peptide in a nonoptimal conformation to form a poorly ordered or "amorphous" deposit corresponds to such a misfolded but low-energy compact state. Subsequently, the peptide/fibril must undergo a reorganization reaction which corresponds, in this isomorphism, with the activated transition from misfolded intermediate to native state protein.

SUMMARY

The proposed energy landscape mechanism for amyloid peptide deposition and β-amyloid fibril growth rests on recent advances in the theory of protein folding and carefully devised laboratory experiments measuring the rate of amyloid fibril elongation. The mechanism incorporates several possible channels for peptide deposition, including (1) fast deposition from solution through an activation/nucleation event, and (2) deposition of peptide from solution onto existing fibrils followed by reorganization of the peptide/fibril deposit. As such, it unifies several views of Aβ peptide deposition and fibril elongation.

The mechanism is consistent with a substantial body of experimental data for the rate of fibril elongation for WT Aβ peptides, Aβ peptide congeners, and mutant Aβ peptide congeners. Moreover, it allows for the clear definitions of equilibrium and kinetic constants, in terms of the energetics of elementary processes of peptide absorption and reorganization, that should be valuable in the interpretation of experimental data for fibril reorganization. The existence of a turnover in the rate of peptide deposition as a function of denaturant concentration or temperature are predicted and may be tested experimentally.

ACKNOWLEDGMENTS

The authors are grateful to Jonathan P. Lee for useful discussions. J.E.S. gratefully acknowledges the National Science Foundation for support and the Center for Computational Science at Boston University.

REFERENCES

1. Selkoe DJ. Alzheimer's disease: a central role for amyloid. J Neuropathol Exp Neurol 1991;53:438–447.
2. Lansbury PT Jr. A reductionist view of Alzheimer's disease. Acc Chem Res 1996;29:317–321.
3. Maggio JE, Mantyh PW. Brain amyloid—a physicochemical perspective. Brain Pathol 1996;6:147–162.
4. Teplow DB. Structural and kinetic features of amyloid β-protein fibrillogenesis. Amyloid Int J Exp Clin Invest 1998;5:121–142.
5. Lomakin A, Chung DS, Benedek GB, Kirscher DA, Teplow DB. On

the nucleation and growth of amyloid β-protein fibrils: detection of nuclei and quantitation of rate constants. Proc Natl Acad Sci USA 1996;93:1125–1129.
6. Lomakin A, Teplow DB, Kirschner DA, Bendek GB. Kinetic theory of fibrillogenesis of amyloid β-protein. Proc Natl Acad Sci USA 1997;94:7942–7947.
7. Naiki H, Gejyo F. Kinetic analysis of amyloid fibril formation. Methods Enzymol 1999;309:305–318.
8. Harper JD, Wong SS, Lieber CM, Lansbury PT Jr. Observation of metastable Aβ amyloid protofibrils by atomic force microscopy. Chem Biol 1997;4:119–125.
9. Walsh DM, Lomakin A, Bendek GB, Condron MM, Teplow DB. Amyloid β-protein fibrillogenesis: detection of a protofibrillar intermediate. J Biol Chem 1997;272:22364–22372.
10. Harper JD, Wong SS, Lieber CM, Lansbury PT Jr. Atomic force microscopic imaging of seeded fibril formation and fibril branching by the Alzheimer's disease amyloid-β protein. Chem Biol 1997;4: 951–959.
11. Esler WP, Stimson ER, Ghilardi JR, Vinters HV, Lee JP, Mantyh PW, Maggio JE. In vitro growth of Alzheimer's disease β-amyloid plaques displays first-order kinetics. Biochemistry 1996;35:749–757.
12. Kusumoto Y, Lomakin A, Teplow DB, Bendek GB. Temperature dependence of amyloid β-protein fibrillization. Proc Natl Acad Sci USA 1998;95:12277–12282. In that article, the diffusion constant is stated to be 1.6×10^{-7} cm^2/s, whereas more recent estimates set it to be an order of magnitude larger 1.4×10^{-6} cm^2/s. With that revised estimate of the diffusion constant, the revised activation energy is $G^{\dagger} = 5.7$ kcal/mol. However, the central conclusion—that the activation entropy is positive—remains unchanged.
13. Esler WP, Felix AM, Stimson ER, Ghiraldi JR, Lu Y-A, Vinters HV, Mantyh PW, Lee JP, Maggio JE. Alzheimer's disease amyloid propagation by a template-dependent dock–lock mechanism. Biochemistry 2000;39:6288–6295.
14. Zhang S, Iwata K, Lachenman MJ, Peng JW, Li S, Stimson ER, Lu YA, Felix AM, Maggio JE, Lee JP. The Alzheimer's peptide Aβ adopts a collapsed coil structure in water. J Struct Biol 2000; 130:130–141.
15. Massi F, Peng JW, Lee JP, Straub JE. Simulation study of the structure and dynamics of the Alzheimer's amyloid peptide congener in solution. Biophys J 2000 (In press).
16. Pechukas P. Statistical approximations in collision theory. In: Miller WH, editor. Dynamics of molecular collisions. Part B. New York: Plenum; 1976. p 269–322.
17. Truhlar DG, Garrett BC, Klippenstein SJ. Current status of transition-state theory. J Phys Chem 1996;100:12771–12800.
18. Berne BJ, Borkovec M, Straub JE. Classical and modern methods in reaction rate theory. J Phys Chem 1988;92:3711–3725.
19. Wolynes PG. Chemical reaction dynamics in complex molecular systems. In: Stein DL, editor. Complex systems. SFI studies in the sciences of complexity. Boston, MA: Addison-Wesley/Longman; 1989. p 355–387.
20. Lee JP, Stimson ER, Ghilardi JR, Mantyh PW, Lu Y-A, Felix AM, Llanos W, Behbin A, Cummings M, Criekinge MV, Timms W, Maggio JE. ^{1}H NMR of Aβ amyloid peptide congeners in water solution. Conformational changes correlate with plaque competence. Biochemistry 1995;34:5191–5200.
21. Zhang SS, Casey N, Lee JP. Residual structure in the Alzheimer's disease peptide: probing the origin of a central hydrophobic cluster. Fold Design 1998;3:413–422.
22. Barrow CJ, Yasuda A, Kenny PT, Zagorksi MG. Solution conformations and aggregational properties of synthetic amyloid β-peptides of Alzheimer's disease—analysis of circular-dichroism spectra. J Mol Biol 1992;225:1075–1093.
23. Jarret JT, Berger EP, Lansbury PT Jr. The carboxy terminus of β amyloid protein is critical for the seeding of amyloid formation: implications for the pathogenesis of Alzheimer's disease. Biochemistry 1993;32:4693–4697.
24. Esler WP, Stimson ER, Fishman JB, Ghilardi JR, Vinters HV, Mantyh PW, Maggio JE. Stereochemical specificity of Alzheimer's disease β-peptide assembly. Biopolymers 1999;49:505–514.
25. Otzen DE, Oliveberg M. Salt-induced detour through compact regions of the protein folding landscape. Proc Natl Acad Sci USA 1999;96:11746–11751.
26. Weissman JS, Kim PS. Reexamination of the folding of BPTI: predominance of native intermediates. Science 1991;253:1386–1393.
27. Camacho C, Thirumalai D. Denaturants can accelerate folding rates in a class of globular proteins. Protein Sci 1996;5:1826–1832.
28. Chan HS, Dill KA. Protein folding in the landscape perspective: chevron plots and non-Arrhenius kinetics. Proteins 1998;30:2–33.
29. Esler WP, Stimson ER, Ghilardi JR, Felix AM, Lu YA, Vinters HV, Mantyh PW, Maggio JE. Aβ deposition inhibitor screen using synthetic amyloid. Nature Biotechnol 1997;15:258–263.
30. Lansbury PT Jr. Evolution of amyloid: what normal protein folding may tell us about fibrillogenesis and disease. Proc Natl Acad Sci USA 1999;96:3342–3344.
31. Thirumalai D, Klimov DK, Woodson SA. Kinetic partitioning mechanism as a unifying theme in the folding of biomolecules. Theor Chem Acc 1997;96:14–22.
32. Onuchic JN, Luthey-Schulten Z, Wolynes PG. Theory of protein folding: the energy landscape perspective. Annu Rev Phys Chem 1997;48:545–600.
33. Wales DJ, Scheraga HA. Global optimization of clusters, crystals, and biomolecules. Science 1999;285:1368–1372.
34. Hao MH, Scheraga HA. Designing potential energy functions for protein folding. Curr Opin Struct Biol 1999;9:184–188.
35. Shakhnoich E, Fersht AR. Folding and binding—overview. Curr Opin Struct Biol 1998;8:65–67.
36. Esler WP, Felix AM, Stimson ER, Lachenmann MJ, Ghilardi JR, Lu YA, Vinters HV, Mantyh PW, Lee JP, Maggio JE. Activation barriers to structural transition determine deposition rates of Alzheimer's disease Aβ amyloid. J Struct Biol 2000;130:174–183.